

# Complexation of diazinon, an organophosphorus pesticide, with $\alpha$ -, $\beta$ -, and $\gamma$ -cyclodextrin — NMR and computational studies<sup>1,2</sup>

Doreen Churchill, Jason Chiu Fung Cheung, Yong Sung Park, Vedene H. Smith, Gary vanLoon, and Erwin Buncel

**Abstract:** Complexation of the organophosphorus pesticide, diazinon, with  $\alpha$ -,  $\beta$ - and  $\gamma$ - cyclodextrin has been investigated through NMR and computational methodologies. Binding constants ( $K_b$ ) determined by  $^1\text{H}$  and  $^{31}\text{P}$  NMR follow the order  $\gamma\text{-CD} > \alpha\text{-CD} = \beta\text{-CD}$ , in contrast with reported  $K_b$  data for other pesticides and thus indicative of steric encumbrance by the isopropyl group in diazinon being an important factor influencing binding constants. The interaction of diazinon with the CDs has also been investigated through computational studies via molecular dynamics – molecular mechanics (MD–MM2) and density functional theory (DFT), B3LYP/6-31G\*. It is shown that the most favorable orientation in binding corresponds to the hydrophobic heterocyclic residue of diazinon being pulled deepest into the CD cavity, in agreement with the experimentally determined order of binding constants. Moreover, the computations show that it is only with  $\gamma$ -CD that the heterocyclic residue of diazinon and the phosphoryl residue are both largely encrypted in the CD cavity, marking a clear differentiation with  $\alpha$ -CD and  $\beta$ -CD where the phosphoryl residue is located largely outside the cavity. Thus, the computational results are in essential agreement with the experimental binding constants where  $\gamma$ -CD stands out with the highest  $K_b$  value. Our work could point to the potential usefulness of computational studies to be undertaken in tandem with experimental work in environmental situations such as soil remediation.

**Key words:** organophosphorus pesticides, diazinon complexation, cyclodextrins, computational studies, molecular mechanics.

**Résumé :** Faisant appel à la RMN et à des calculs théoriques, on a étudié la complexation du diazinon, un pesticide organophosphoré, avec les  $\alpha$ -,  $\beta$ - et  $\gamma$ -cyclodextrines. Faisant appel à la RMN du  $^1\text{H}$  et du  $^{31}\text{P}$ , on a déterminé que les constantes de fixation ( $K_b$ ) sont dans l'ordre  $\gamma\text{-CD} > \alpha\text{-CD} = \beta\text{-CD}$ , ce qui contraste avec les valeurs de  $K_b$  rapportées pour d'autres pesticides; ces différences pourraient suggérer que l'encombrement stérique provoqué par le groupe isopropyle du diazinon est un facteur qui présente une influence importante dans les constantes de fixation. L'interaction du diazinon avec les cyclodextrines a été examinée d'une façon théorique en faisant appel à la théorie de la dynamique moléculaire – mécanique moléculaire (DM–MM2) et à la théorie de la densité fonctionnelle (TDF), B3LYP/6-31G\*. On a montré que l'orientation la plus favorable lors de la fixation correspond à celle où le résidu hétérocyclique hydrophobe du diazinon est inséré au point le plus profond de la cavité de la cyclodextrine, ce qui correspond à l'ordre déterminé d'une façon expérimentale par les constantes de fixation. De plus, les calculs montrent le résidu hétérocyclique du diazinon et le résidu phosphoryle ne sont bien insérés que dans la cavité de la  $\gamma$ -CD, ce qui la différencie clairement de l' $\alpha$ -CD et de la  $\beta$ -CD avec lesquelles le résidu phosphoryle se trouve largement à l'extérieur de la cavité. Les résultats théoriques sont donc, pour l'essentiel, en accord avec les constantes de fixations expérimentales alors que la valeur pour la  $\gamma$ -CD est la plus élevée. Ce travail pourrait démontrer l'utilité potentielle d'études théoriques pour étudier, en tandem, avec des expérimentales, des situations environnementales, telles que la récupération des sols.

**Mots clés :** pesticides organophosphorés, complexation du diazinon, cyclodextrines, études théoriques, mécanique moléculaire.

[Traduit par la Rédaction]

Received 6 December 2005. Published on the NRC Research Press Web site at <http://canjchem.nrc.ca> on 13 May 2006. Reposted on the Web site with correction on 16 May 2006.

*This paper is dedicated to Professor Walter Szarek in recognition of his contributions to chemistry.*

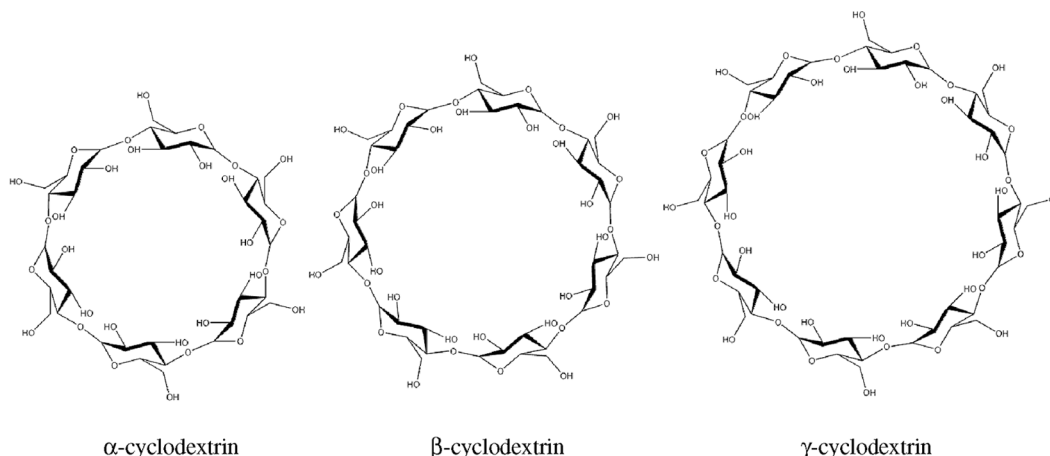
**D. Churchill.** Centre of Environmental Excellence, c/o Sir Wilfred Grenfell College, Corner Brook, NF A2H 6P9, Canada.  
**J.C.F. Cheung, Y.S. Park, V.H. Smith,<sup>3</sup> G. vanLoon, and E. Buncel.<sup>4</sup>** Department of Chemistry, Queen's University, Kingston, ON K7L 3N6, Canada.

<sup>1</sup>This article is part of a Special Issue dedicated to Professor Walter A. Szarek.

<sup>2</sup>Part 9 in a series titled "Mechanisms of abiotic degradation and soil–water interactions of pesticides and other hydrophobic organic compounds". For part 8, see ref. 1.

<sup>3</sup>Deceased.

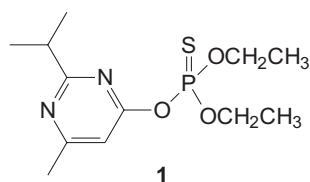
**Fig. 1.** Chemical structure of  $\alpha$ -CD,  $\beta$ -CD, and  $\gamma$ -CD consisting of six, seven, and eight glucose units, respectively.



## Introduction

The wide usage of pesticides in modern agriculture, coupled with the known toxicity of pesticide residues to humans and other nontarget organisms, calls for fresh research into methods for the facile degradation of such residues under environmentally benign conditions and without generating further toxic materials (metabolites) in the process. Our own approach toward that goal is through the tools of structure–reactivity relationships in physical organic chemistry and environmental science. Several papers have been published from our laboratories concerning the degradation of various pesticides and other hydrophobic organic compounds (1–7).

In the present work we have explored, through computational and NMR methodology, the interaction of the organophosphorus pesticide, diazinon (**1**), with several cyclodextrin (CD) molecules.



The CDs being investigated are  $\alpha$ -,  $\beta$ -, and  $\gamma$ -CD, containing six, seven, and eight glucose moieties, respectively, in the cyclic structure (Fig. 1). The CDs may be shown by the torus (“bucket”) representation in which the secondary hydroxyls are situated on the upper, wider rim, and the primary hydroxyls on the lower rim (see figures in the Computational studies section).

The important characteristic of the CD-type glucose oligosaccharide structure is a hydrophilic exterior imparted by the CD hydroxyl groups and an interior lined by H-C-O linkages that impart hydrophobic character (8, 9). The hydrophobic interior is then capable of encapsulating a hydrophobic or low polarity molecule, for example, a typical pesticide containing an aromatic or heteroaromatic moiety, resulting in the formation of a host–guest complex. The driving force for CD host–guest complex formation is presumed to have as its origin the combination of the following factors: (1) release of “high-energy”  $\text{H}_2\text{O}$  molecules from the CD cavity; (2) relief of strain in the CD molecule upon

complexation of the guest (important for the small  $\alpha$ -CD); (3) hydrophobic and van der Waals interactions; (4) hydrogen bonding between host and guest; (5) compatibility between guest size and dimensions of the host cavity; (6) orientation of the guest molecule in the cavity. The computer modeling and NMR studies reported in this paper bring insight into some of these factors.

CDs have a potentially uniquely important role in the removal of pesticide residues from contaminated soils, for example, from localized industrial sites. In such a situation, the leaching of the pesticide through rainwater, along with other hydrophobic compounds, causes these to localize below the ground water table where they accumulate as DNPLs (dense nonaqueous phase liquids); there they remain virtually immune to degradation through bacterial action over several decades or longer (10). Now, if a CD solution is pumped from the surface into the DNPL, it complexes the hydrophobic material, which once solubilized, can be carried downstream. From there it can be pumped up to the surface where it is separated into its constituents and degraded, while the CD solution is recycled upstream. This process is similar to the traditional “pump-and-treat” procedure using surfactants (11).

Measurement of binding constants between a given pesticide and available CDs enables one to quantify and optimize this methodology. Different methods for the determination of binding constants have been developed (8, 9, 12), including NMR spectroscopy (13, 14). In the case of diazinon, both  $^1\text{H}$  and  $^{31}\text{P}$  NMR become particularly convenient.

## Experimental

### Materials

Diazinon was synthesized based on the method of Gysin and Margot (15). The dried sodium salt of 2-isopropyl-6-methylpyrimidin-4-ol was heated for 2 days under nitrogen with diethyl chlorothiophosphate in dry acetone at  $35^\circ\text{C}$ . After cooling and filtering to remove KCl, then removal of solvent under vacuo, the residue was chromatographed with methylene chloride as eluent. Further purification was effected by dissolving in hexanes and extracting with water. The hexane layer was dried ( $\text{MgSO}_4$ ), and after filtering was first concentrated and then dried in vacuo to yield pure diazinon. Purity was checked by  $^1\text{H}$ ,  $^{13}\text{C}$  (proton-decoupled),

and  $^{31}\text{P}$  (proton-decoupled) NMR. Spectra were run on a 300 MHz Bruker Avance spectrophotometer using  $\text{CDCl}_3$  as solvent. All spectra were consistent with diazinon and contained no impurity peaks.  $^1\text{H}$  NMR (ppm)  $\delta$ : 6.64 (s, 1H), 4.33 (d of q,  $J_{\text{H-H}} = 7.1$  Hz,  $J_{\text{H-P}} = 11.2$  Hz, 4H), 3.10 (sept,  $J_{\text{H-H}} = 6.9$  Hz, 1H), 2.47 (s, 3H), 1.37 (t,  $J_{\text{H-H}} = 7.1$  Hz, 6H), 1.30 (d,  $J_{\text{H-H}} = 6.9$  Hz, 6H).  $^{13}\text{C}$  NMR (ppm)  $\delta$ : 176 (s), 170(s), 165 (d,  $J_{\text{C-P}} = 4.6$  Hz), 107 (d,  $J_{\text{C-P}} = 6.4$  Hz), 65.6 (d,  $J_{\text{C-P}} = 5.1$  Hz), 37.7 (s), 24.5 (s), 21.8 (s), 16.2 (d,  $J_{\text{C-P}} = 8.0$  Hz).  $^{31}\text{P}$  NMR (ppm)  $\delta$ : 61 (s).

$\alpha$ -,  $\beta$ -, and  $\gamma$ -CDs were a generous gift from Cerestar USA and were used without further treatment.  $\text{DMSO-}d_6$  and  $\text{D}_2\text{O}$  were purchased from Cambridge Isotopes and used as received.

## NMR determination of binding constants

### Sample preparation

To determine each binding constant, 10 samples were prepared in NMR tubes; the first with diazinon (plus  $\text{DMSO}$  cosolvent, 0.2% v/v) in  $\text{D}_2\text{O}$ , and the following containing successively more CD. First, a 0.99 mol/L stock solution of diazinon was prepared in  $\text{DMSO-}d_6$ , then a 0.006–0.06 mol/L stock solution of CD in 2.5 mL  $\text{D}_2\text{O}$ . Ten NMR tubes were filled with various amounts of the CD solution and  $\text{D}_2\text{O}$  to give a range of CD concentrations from zero ( $\text{D}_2\text{O}$  only) to that of the pure CD stock solution (no added  $\text{D}_2\text{O}$ ). To each tube was added 2.5  $\mu\text{L}$  of the diazinon stock solution, giving a final diazinon concentration of  $4.93 \times 10^{-3}$  mol/L in each. The NMR spectra were recorded using a 400 or 500 MHz Bruker Avance spectrophotometer.

### $K_b$ determination by $^1\text{H}$ NMR

$^1\text{H}$  NMR spectra were run on all 10 tubes using a water presat to remove the HOD peak from the spectra. Two proton signals were examined, the aromatic proton (Ar-H) on the pyrimidinol ring and the  $\text{CH}_3$  protons (Ar-Me) located on the pyrimidinol ring, as illustrated in Fig. 2. Both singlets appear in an area of the spectrum with no interference from CD signals. The change in chemical shift ( $\Delta\delta$ ) for the Ar-Me and Ar-H peaks of diazinon with increasing CD concentration, when plotted against [CD], yielded a curved binding isotherm. The curve-fitting program GraphPad Prism<sup>®</sup> was used to determine  $K_b$  according to eq. [1]

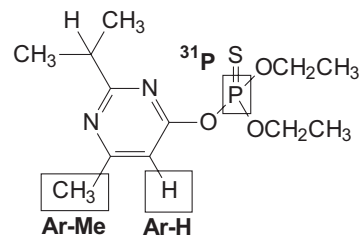
$$[1] \quad \Delta = \frac{\Delta_b K_b [\text{CD}]}{1 + [\text{CD}] K_b}$$

where  $\Delta$  is the observed change in chemical shift,  $\Delta_b$  is the maximum change in chemical shift for 100% bound substrate, and  $K_b$  is the binding constant.  $K_b$  values were also obtained by the Benesi–Hildebrand eq. [2], the linear double reciprocal plot of the binding isotherm equation.

$$[2] \quad \frac{1}{\Delta} = \frac{1}{\Delta_b K_b [\text{CD}]} + \frac{1}{\Delta_b}$$

On plotting  $1/\Delta$  vs.  $1/[\text{CD}]$ ,  $K_b$  was found by dividing the intercept by the slope, as determined by linear regression using Microsoft Excel<sup>®</sup>. Each determination was made at least twice by each method, and all of the values acquired were averaged to obtain the reported  $K_b$  value.

**Fig. 2.** Structure of diazinon illustrating the portions studied by NMR to determine the binding constant ( $K_b$ ) with cyclodextrins.



### $K_b$ determination by $^{31}\text{P}$ NMR

Proton-decoupled  $^{31}\text{P}$  NMR spectra were recorded for each tube (see the general Sample preparation section), as singlets, no other peaks being observed. The change in chemical shift ( $\Delta\delta$ ) with increasing CD concentration gave a curved binding isotherm. Plotting  $\Delta\delta$  vs. [CD] and using the curve-fitting program GraphPad Prism<sup>®</sup> yielded  $K_b$  according to eq. [1].  $K_b$  was again evaluated using the Benesi–Hildebrand eq. [2]. Each determination was made at least twice by each method, and all of the acquired values were averaged to obtain the reported  $K_b$  value.

## Results and discussion

### CD–diazinon binding constants

#### $K_b$ from $^1\text{H}$ NMR

The change in chemical shift of the Ar-H and Ar-Me peaks in the NMR spectra of diazinon on increasing the CD concentration was followed for  $\alpha$ -,  $\beta$ -, and  $\gamma$ -CD. The change in chemical shift was downfield, except for the Ar-H peak in  $\gamma$ -CD, where it shifted upfield with increasing [CD]. The data were used to produce binding isotherms that fit a 1:1 binding model for all three CDs. Figure 3 shows results for  $\alpha$ -CD. Figure 3a gives the binding isotherm generated for the Ar-H peak, which yields  $K_b = 183$  (mol/L)<sup>-1</sup>, while Fig. 3b provides the plot according to the Benesi–Hildebrand treatment, yielding  $K_b = 221$  (mol/L)<sup>-1</sup>. Plots for  $\beta$ -CD and  $\gamma$ -CD are qualitatively similar.

#### $K_b$ from $^{31}\text{P}$ NMR

Downfield changes in the  $^{31}\text{P}$  NMR chemical shift for diazinon were observed on increasing the CD concentration for  $\alpha$ -,  $\beta$ -, and  $\gamma$ -CD. Figure 4a shows the binding isotherm for  $\alpha$ -CD, while Fig. 4b gives the Benesi–Hildebrand plot of the data.  $\beta$ -CD and  $\gamma$ -CD yield similar plots.

### Structure–stability relationships

The overall average  $K_b$  values obtained from the  $^1\text{H}$  (Ar-H and Ar-Me) and  $^{31}\text{P}$  NMR data are given in Table 1. Clearly, the largest  $K_b$  value is found for  $\gamma$ -CD, around 400 (mol/L)<sup>-1</sup>, while the values for  $\alpha$ -CD and  $\beta$ -CD are not significantly different, at around 200 (mol/L)<sup>-1</sup>.

A partial summary of existing literature  $K_b$  data for pesticides is given in Table 2. The values generally vary from 100 to 600 (mol/L)<sup>-1</sup>. Thus, the present results for diazinon (Table 1) fall within the range of existing data for other pesticides (Table 2). Data for all three CDs are available for parathion (2), methyl parathion (3), and paraoxon (4), all three organophosphorus pesticides with an aromatic moiety

**Fig. 3.** (A) Binding isotherm and (B) Benesi–Hildebrand plots for the binding of diazinon with  $\alpha$ -CD generated from  $^1\text{H}$  NMR data for the Ar-H peak.

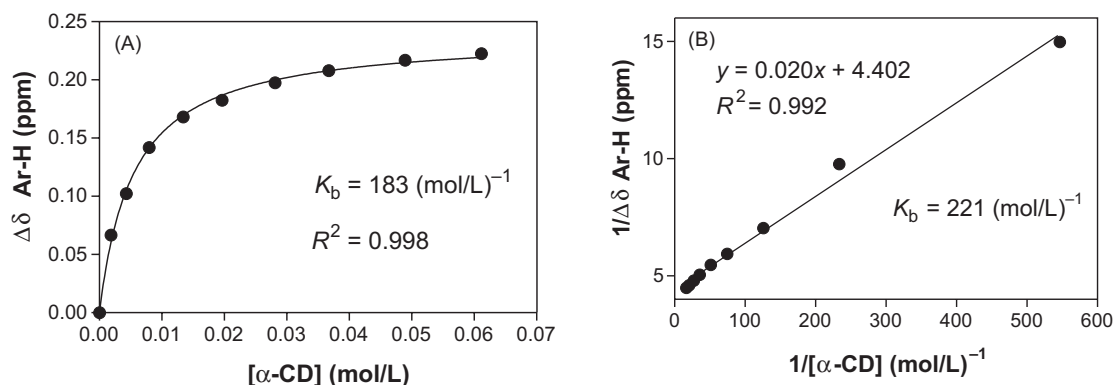
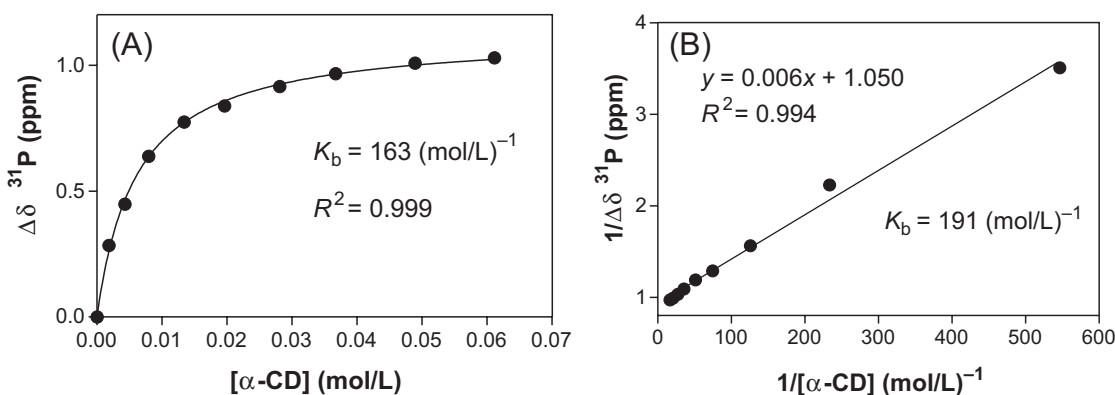
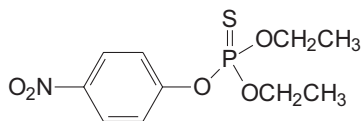


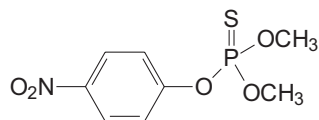
**Fig. 4.** (A) Binding isotherm and (B) Benesi–Hildebrand plots for the binding of diazinon with  $\alpha$ -CD generated from  $^{31}\text{P}$  NMR data.



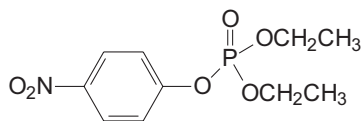
in place of the heteroaromatic moiety in diazinon, but otherwise similar structures.



2



3



4

A major difference between our results and earlier ones now becomes apparent in that  $K_b$  values in Table 2 are lowest for  $\gamma$ -CD, while in our study (Table 1),  $\gamma$ -CD has the

highest  $K_b$ . A plausible explanation for this variance lies with the sterically demanding isopropyl group in diazinon, which together with the Ar-methyl cannot easily be accommodated in the  $\alpha$ -CD or  $\beta$ -CD cavity, but can be readily accommodated in the  $\gamma$ -CD cavity. The computational study that follows sheds further light on this aspect.

### Computational studies

The manifold applications of computational chemistry have made enormous impact in the field of cyclodextrin chemistry, including modeling studies of the host–guest type. The article by Kenny Lipkowitz on this subject, which appeared in 1998 in a special issue of *Chemical Reviews* featuring cyclodextrin chemistry, provides an excellent overview of this area up to that time; it lists 214 references (24), while many have appeared since then. In this study we present results of two approaches in computational chemistry as applicable to the present system: molecular mechanics (MM) and ab initio, density functional theory (DFT).

### B3LYP energy optimized structures

Figure 5 presents the B3LYP/6-31G\*\* minimized structure of diazinon in the form of the space-filling model and as ball-and-stick representation. These are used in visualizing the orientations of diazinon bound in the  $\alpha$ -,  $\beta$ -, and  $\gamma$ -CD cavities presented in the following.

### Binding orientations of diazinon into $\alpha$ -, $\beta$ -, and $\gamma$ -CDs

The dimensions of the diazinon – CD bound complex have been evaluated using MD–MM2 and the results are

**Table 1.** Diazinon-CD binding constants ( $K_b$ , (mol/L)<sup>-1</sup>) determined by <sup>1</sup>H and <sup>31</sup>P NMR.

CD	Average $K_b$ ((mol/L) <sup>-1</sup> ) <sup>a</sup> determined by Ar-H <sup>1</sup> H NMR		Average $K_b$ ((mol/L) <sup>-1</sup> ) <sup>a</sup> determined by Ar-Me <sup>1</sup> H NMR		Average $K_b$ ((mol/L) <sup>-1</sup> ) <sup>a</sup> determined by <sup>31</sup> P NMR		Average $K_b$ from all methods
	Binding isotherm	Benesi-Hildebrand	Binding isotherm	Benesi-Hildebrand	Binding isotherm	Benesi-Hildebrand	
$\alpha$ -CD	181±3	220±1	200±0	283±54	157±8	179±18	203±46
$\beta$ -CD	200±0	156±14	200±0	215±45	134±35	121±31	170±45
$\gamma$ -CD	422±32	368±41	456±16	335±30	454±33	328±38	390±63

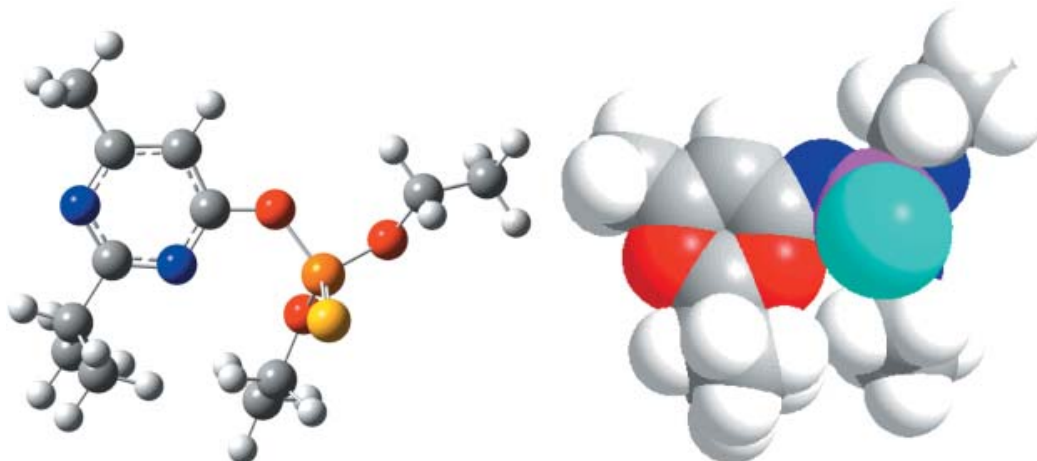
<sup>a</sup>Error limits in the  $K_b$  value were taken as the standard deviation (three or more values) or the average deviation (only two values).

**Table 2.** Binding constants of different pesticides with  $\alpha$ -CD,  $\beta$ -CD, and  $\gamma$ -CD.

Pesticide	$\alpha$ -CD <sup>a</sup> $K_b$ ((mol/L) <sup>-1</sup> )	$\beta$ -CD <sup>a</sup> $K_b$ ((mol/L) <sup>-1</sup> )	$\gamma$ -CD <sup>a</sup> $K_b$ ((mol/L) <sup>-1</sup> )	Ref.
Diazinon	203±46	170±45	390±63	This work
Parathion	—	526	—	16
	—	286	—	17
	588	192	83	18
Paraoxon	123	182	110	18
Methyl parathion	285	526	119	18
	—	625	—	16
	—	526	—	17
Fenitrothion	—	417	—	16
	—	227	—	17
Pirimiphos-methyl	—	171±34	—	19
Chlorpyrifos	—	90±28	—	19
DCPE <sup>b</sup>	—	555	—	20
(S)-(+)-Sarin	167±25	—	—	21
(S)-(-)-Sarin	25±2	—	—	21
Warfarin	—	160	—	22
Coumatetraly	—	565±42	—	19
Carbaryl	—	289±21	—	23
Deltamethrin	—	627±104	—	19
Fenvalerate	—	316±46	—	19

<sup>a</sup> $K_b$  error limits listed as available in the referenced paper.

<sup>b</sup> $\alpha$ -(Diethoxyphosphinoximino)dicyclopropylmethane (DCPE).

**Fig. 5.** Ball-and-stick (left) and space-filling model (right) of diazinon optimized with B3LYP/6-31G\*\*.

**Fig. 6.**  $\alpha$ -CD-,  $\beta$ -CD-, and  $\gamma$ -CD-diazinon binding orientation, energy optimized with MD-MM2. Top row shows the diazinon in the ball-and-stick model and the  $\alpha$ -CD,  $\beta$ -CD, and  $\gamma$ -CD in the wire-frame model; bottom row shows the torus representation of  $\alpha$ -CD,  $\beta$ -CD, and  $\gamma$ -CD.

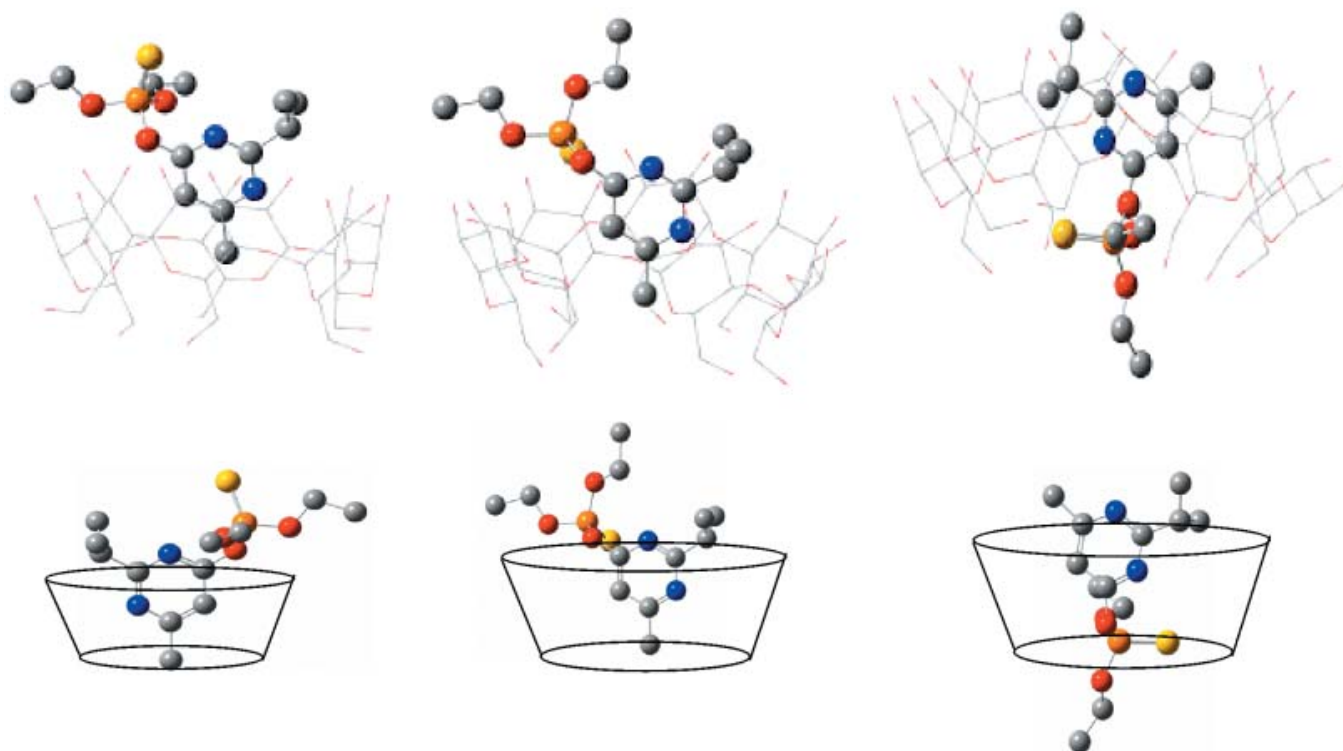


**Table 3.** Primary OH rim radius, secondary OH rim radius, and height of the diazinon-CD complexes, with errors, optimized with MD-MM2.

	Primary OH rim radius (Å)	Error in primary rim radius (Å)	Secondary OH rim radius (Å)	Error in secondary radius (Å)	Height (Å)	Error in height (Å)
$\alpha$ -CD + diazinon	4.97	1.25	5.13	1.00	5.24	0.41
$\beta$ -CD + diazinon	5.77	1.62	6.25	0.85	5.40	0.47
$\gamma$ -CD + diazinon	5.57	1.45	6.76	1.31	5.86	0.39

given in Table 3 as the primary OH rim and secondary OH rim radii, and the height of the complexed CDs. The diazinon-complexed  $\gamma$ -CD is found to have the largest secondary OH rim radius, as expected. Interestingly however, the primary OH rim radius in the complexed CD is about equal for  $\beta$ - and  $\gamma$ -CD.

We have also calculated (using MM2) the distance from the phosphorus atom of diazinon to the secondary OH rim, as the average distance to the three nearest secondary oxygen neighbours. This gives a measure of the depth of the diazinon molecule inside the CD cavity. The results given in Table 4 clearly show that this distance is greatest with  $\gamma$ -CD, i.e., diazinon is found deepest in the CD cavity with  $\gamma$ -CD.

Figure 6 shows the different orientations for the binding of diazinon in  $\alpha$ -,  $\beta$ -, and  $\gamma$ -CD optimized with MD-MM2. The illustrations given are for both ball-and-stick models showing diazinon inside the wire-frame CD and the corresponding CD torus representation (Fig. 6), and also space-filling models (Fig. 7).

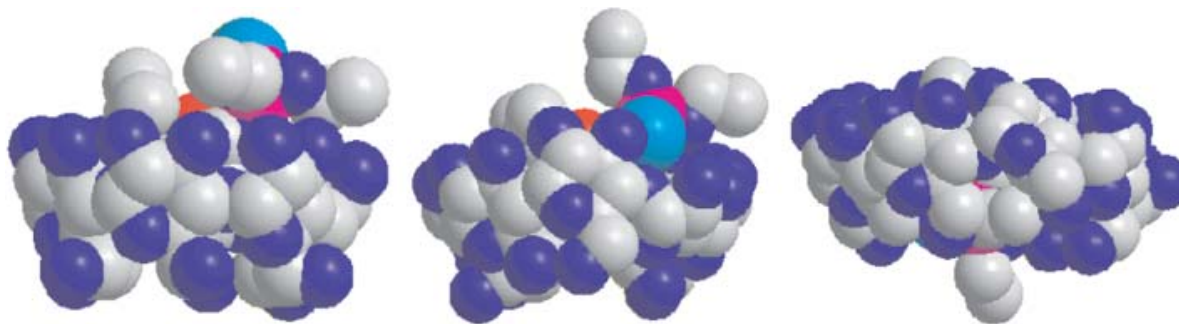
**Table 4.** Calculation of average distance from the phosphorus atom to the secondary oxygen plane optimized with MM2 with three nearest oxygen neighbours.

	Distance (Å)
$\alpha$ -CD + diazinon	2.52
$\beta$ -CD + diazinon	0.55
$\gamma$ -CD + diazinon	6.37

**Note:** Alternatively one can indicate distance measurements above the rim as + and below the rim as -, giving the values for  $\alpha$ -CD (+2.52),  $\beta$ -CD (+0.55),  $\gamma$ -CD (-6.37).

Several important observations follow on visual examination of these models. (1) The heterocyclic residue of diazinon appears inside the cavity for all three CDs. (2) The methyl substituent is inside the cavity and points downwards for  $\alpha$ - and  $\beta$ -CD, while for  $\gamma$ -CD it is situated largely out-

Fig. 7. Space-filling model of diazinon with  $\alpha$ -,  $\beta$ -, and  $\gamma$ -cyclodextrins complex optimized with MD-MM2.



side, pointing upwards. (3) The isopropyl substituent is largely outside pointing upwards for  $\alpha$ - and  $\beta$ -CD, while being situated on the secondary rim with  $\gamma$ -CD (4). The main contrast comes with the phosphoryl residue that is essentially outside the cavity for  $\alpha$ - and  $\beta$ -CD, while with  $\gamma$ -CD it is inside the cavity, with the exception of one ethoxy substituent that protrudes from the lower rim.

Thus, the computations reveal a clear contrast in the three computed orientations. In the case of  $\gamma$ -CD, the bulk of the hydrophobic diazinon molecule, i.e., both the heterocyclic residue and the phosphoryl residue, are situated inside the CD cavity, whereas with  $\alpha$ - and  $\beta$ -CD only the heterocyclic residue is present inside the cavity. This, then, provides a rationale for the experimental observation of  $\gamma$ -CD having the greatest binding constant compared with  $\alpha$ -CD and  $\beta$ -CD, which possess much smaller and virtually equal  $K_b$  values. Any attempts at environmental remediation of pesticides, e.g., from soils, must be cognizant of these findings.

### Concluding comments

Binding of the organophosphorus pesticide, diazinon, to  $\alpha$ -,  $\beta$ -, and  $\gamma$ -cyclodextrin has been investigated through NMR and computational methodologies. The largest  $K_b$  value ( $400 \text{ (mol/L)}^{-1}$ ) was observed for  $\gamma$ -CD ( $^1\text{H}$  and  $^{31}\text{P}$  NMR). This was corroborated computationally (MD-MM2 and B3LYP/6-31\*\*), which have revealed the deepest location for the hydrophobic diazinon molecule within  $\gamma$ -CD. The direct correspondence and mutually supporting nature of the experimental and computational results, suggests a promising role for computational methodology in environmental remediation of pesticides.

### References

- V.K. Balakrishnan, E. Buncel, and G.W. vanLoon. *Environ. Sci. Technol.* **39**, 5824 (2005).
- V.K. Balakrishnan, X. Han, G.W. vanLoon, J.M. Dust, J. Toullec, and E. Buncel. *Langmuir*, **20**, 6586 (2004).
- S. Shirin, E. Buncel, and G.W. vanLoon. *Can. J. Chem.* **81**, 45 (2003).
- V.K. Balakrishnan, J.M. Dust, G.W. vanLoon, and E. Buncel. *Can. J. Chem.* **79**, 157 (2001).
- J.E. Omakor, I. Onyido, G.W. vanLoon, and E. Buncel. *J. Chem. Soc. Perkin Trans. 2*, 324 (2001).
- G.W. vanLoon and S. Duffy. *Environmental chemistry: A global perspective*. Oxford University Press, New York, 2000.
- M.T. Annandale, G.W. VanLoon, and E. Buncel. *Can. J. Chem.* **76**, 873 (1998).
- M.L. Bender and M. Komiyama. *Cyclodextrin chemistry*. Springer-Verlag, Berlin, Heidelberg, New York, 1978.
- J. Szejtli and T. Osa (*Editors*). *Comprehensive supramolecular chemistry*. Vol. 3. Cyclodextrins. Elsevier Science, Ltd., New York, 1996.
- (a) T.B. Boving, X. Wang, and M.L. Brusseau. *Environ. Sci. Technol.* **33**, 764 (1999); (b) M.L. Brusseau, X. Wang, and W. Wang. *Environ. Sci. Technol.* **31**, 1087 (1997); (c) J.E. McCray and M.L. Brusseau. *Environ. Sci. Technol.* **33**, 89 (1999); (d) J.E. Morillo, J.I. Pérez-Martinez, and J.M. Ginés. *Chemosphere*, **44**, 1065 (2001).
- (a) D.A. Sabatini, R.C. Knox, and J.H. Harwell (*Editors*). *Surfactant-enhanced subsurface remediation-emerging technologies*. ACS Symposium Series 594. American Chemical Society, Washington, D.C. 1995; (b) D.F. Lowe, C.L. Oubre, and C.H. Ward. *Surfactants and cosolvents for NAPL remediation — A technology practices manual*. Lewis Publishers, Boca Raton, Florida, 1999.
- (a) K.A. Connors. *Chem. Rev.* **97**, 1325 (1997); (b) K.A. Connors. *Binding constants*. John Wiley and Sons Inc., Toronto, 1987.
- L. Fielding. *Tetrahedron*, **56**, 6151 (2000).
- H.-J. Schneider, F. Hacket, and V. Rüdiger. *Chem. Rev.* **98**, 1755 (1998).
- H. Gysin and A. Margot. *J. Agric. Food Chem.* **6**, 900 (1958).
- M. Kamiya and K. Nakamura. *Pestic. Sci.* **41**, 305 (1994).
- M. Kamiya, K. Nakamura, and C. Sasaki. *Chemosphere*, **30**, 653 (1995).
- M. Kamiya, S. Mitsuhashi, and M. Makino. *Chemosphere*, **25**, 1783 (1992).
- A. Coly and J.-J. Aaron. *Anal. Chim. Acta*, **360**, 129 (1998).
- Y.L. Loukas, E.A. Vyza, and A.P. Valiraki. *Analyst (Cambridge, U.K.)*, **120**, 533 (1995).
- C. Van Hooendonk and J.C.A.E. Breebaart-Hansen. *Recl. Trav. Chim. Pays-Bas*, **89**, 289 (1970).
- J.C. Marquez, M. Hernandez, and F. Garcia Sanchez. *Analyst (Cambridge, U.K.)*, **115**, 1003 (1990).
- F. Barbato, M.I. La Rotonda, A. Miro, P. Morrica, and F. Quaglia. *J. Inclusion Phenom. Macrocyclic Chem.* **38**, 423 (2000).
- K.B. Lipkowitz. *Chem. Rev.* **98**, 1829 (1998).